Colliding pulse injection of polarized electron bunches in a laser-plasma accelerator

S. Bohlen [1], Z. Gong [2], M. J. Quin [2], M. Tamburini [2] and K. Põder [1,*]
[1]*Deutsches Elektronen-Synchrotron DESY, Notkestraße 85, 22607 Hamburg, Germany*
[2]*Max-Planck-Institut für Kernphysik, Saupfercheckweg 1, 69117 Heidelberg, Germany*

(Received 5 April 2023; accepted 28 August 2023; published 22 September 2023)

Highly polarized, multi-kiloampere-current electron bunches from compact laser-plasma accelerators are desired for numerous applications. Current proposals to produce these beams suffer from intrinsic limitations to the reproducibility, charge, beam shape, and final polarization degree. In this paper, we propose colliding pulse injection (CPI) as a technique for the generation of highly polarized electron bunches from prepolarized plasma sources. Using particle-in-cell simulations, we show that colliding pulse injection enables trapping and precise control over electron spin evolution, resulting in the generation of high-current (multi-kA) electron bunches with high degrees of polarization (up to 95% for >2 kA). Bayesian optimization is employed to optimize the multidimensional parameter space associated with CPI to obtain a percent-level energy spread, submicron normalized emittance electron bunches with 90% polarization using 100-TW class laser systems.

DOI: 10.1103/PhysRevResearch.5.033205

I. INTRODUCTION

Spin-polarized electron beams are of fundamental importance in atomic, nuclear, and particle physics [1–4] due to the possibility of increasing the sensitivity of fundamental processes and enabling results competing with high-energy accelerators [5]. As such, polarized beams are also considered in many proposals for future colliders [6], e.g., to enhance the searches at these machines for physics beyond the standard model [7]. Furthermore, polarized electrons can be used to generate polarized beams of photons [8] or positrons [9], which are of great interest in material science applications [10].

Currently, the main sources of polarized electron beams are storage rings relying on radiative polarization (the Sokolov-Ternov effect) [11] and polarized photocathodes [12]. These machines rely on radio-frequency (rf) technology and are therefore large scale and scarce. Laser-plasma acceleration (LPA) [13,14] offers an exciting alternative to conventional accelerator technology by utilizing 100-GV/m-level acceleration gradients in plasma waves excited by an ultrahigh laser pulse in a tenuous plasma. Alternative sources of polarized beams have been proposed [15,16], including techniques to create spin-polarized electron beams with orders of magnitude higher peak currents than rf sources with compact LPAs. Concepts such as generation of polarized beams from prepolarized plasma sources using density down-ramp injection (DDR) [17], self-injection (SI) [18], or Laguerre-Gaussian (LG) laser beams [19] have been put forward. Several proposals also exist for employing beam-driven plasma accelerators [20–22] or interactions with ultrahigh-intensity laser pulses [23–27] to generate spin-polarized electron bunches.

Among these novel polarized electron beam source proposals, LPA-based concepts show the highest near-term potential. Yet all currently proposed methods suffer from limitations hindering their practical implementation. The azimuthal magnetic field inside the LPA acceleration cavity decreases the polarization of electrons injected off axis in the DDR case, limiting the driver laser to $a_0 \lesssim 1$ and consequently the charge of highly polarized electron bunches to hundreds of femtocoulomb [17]. Here, $a_0 \simeq 0.85\lambda_0(\mu\mathrm{m})\sqrt{I_0(10^{18}\ \mathrm{W\,cm^{-2}})}$ is the peak normalized laser vector potential, where λ_0 and I_0 are the laser wavelength and peak intensity, respectively. Furthermore, the low a_0 necessitates very sharp density transitions, which are difficult to generate. Studies have shown that highly spin-polarized beams can be self-injected, but deviations from perfect spherical symmetry will severely downgrade beam polarization [18]. And while high current and polarization can be achieved using LG laser drivers, the resulting annular electron beams can be impractical and very sharp density transitions are again required [19].

In this paper, we propose using colliding pulse injection (CPI) [28–30] to create highly polarized (>90%), high charge (tens of pC), and low normalized emittance (<1 mm mrad) electron beams with percent-level energy spread from a prepolarized plasma source. The easily adjustable degrees of freedom stemming from the colliding laser pulse properties enable control over the phase-space volume of the injected bunch and spin depolarization during the injection process. We employ Bayesian optimization [31,32] to tune some of the available degrees of freedom to demonstrate the generation of high-quality, highly polarized electron bunches, thereby exemplifying the huge potential of this technique.

*kristjan.poder@desy.de

Published by the American Physical Society under the terms of the Creative Commons Attribution 4.0 International license. Further distribution of this work must maintain attribution to the author(s) and the published article's title, journal citation, and DOI.

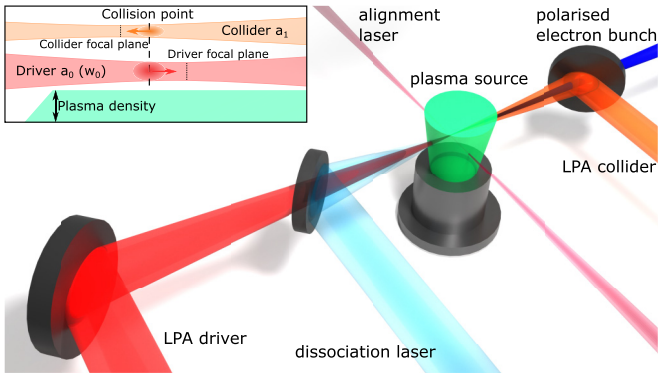

FIG. 1. Schematic setup of a laser plasma accelerator employing CPI for the generation of spin-polarized electron beams from a prepolarized plasma source; the different laser beams are discussed in the main text. The inset shows parameters that can be varied to optimize the injected electron bunch parameters: plasma density n_e, collision point z_c, focal plane $z_{f,0}$ ($z_{f,1}$), and intensity a_0 (a_1) of the driver (collider) laser.

II. POLARIZATION IN COLLIDING PULSE INJECTION

A schematic setup for polarized LPA using CPI is shown in Fig. 1. CPI employs a second laser pulse (orange) counterpropagating to the LPA driver (red), with the standing wave set up in the vicinity of their collision point enabling trapping of background electrons.

The plasma source could be prepolarized using hydrogen halide molecular dissociation [33–38]. A subnanosecond alignment laser perpendicular to the LPA driver (purple) aligns the molecular bonds. Subsequently a circularly polarized UV pulse (teal) dissociates the halide molecule, resulting in two polarized valence electrons from the hydrogen-halide bond. After full ionization of outer shell electrons this would result in a maximum polarization of 25% for hydrogen halides. The delay from dissociation to injection into the wakefield must be of the order of tens of picoseconds, much smaller than the time for hyperfine coupling transferring polarization from electrons to nucleus [36]. To increase the prepolarization degree towards 100%, the dissociated hydrogen atoms with their spin-polarized electrons could be spatially separated from the halide atoms via resonance-enhanced multiphoton ionization of the halide atoms [19,39] or other methods [40]. Alternatively, the prepolarization technique could potentially be extended to pure hydrogen in the future, e.g., using lasers with $\lambda \lesssim 100\,\text{nm}$ for the dissociation, which are only recently becoming available [41], or other developments that enable the production of spin-polarized hydrogen. In an experiment, only the restricted volume where electrons are trapped must be prepolarized. CPI is greatly advantageous as the location of the collision point can easily be adjusted to this prepolarized volume; indeed, a micron-scale overlap of multiple laser pulses at arbitrary positions in a plasma has already been demonstrated [42]. In this paper, we assume a 100% prepolarized plasma source to study the achievable spin polarization using CPI.

Bunch injection in CPI can be described in terms of electron trapping, utilizing the Hamiltonian $\mathcal{H}(p_z, \xi)$ inside the potential well of a nonlinear plasma wave [43,44], where

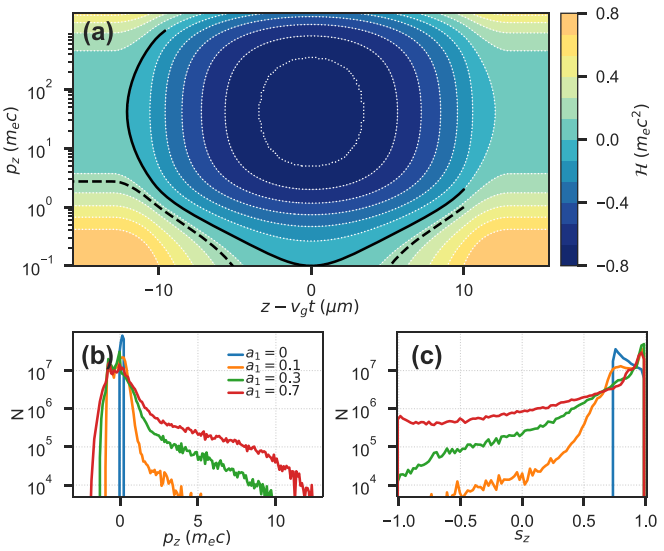

FIG. 2. (a) The Hamiltonian of a test electron in a plasma wave, showing an untrapped (dashed line) and trapped (solid line) orbit. (b) Longitudinal momentum distribution of test electrons with $r < w_1$ after interacting with a collider pulse of varying intensity in vacuum, showing the onset and increase of stochastic electron heating. (c) Histogram of s_z after an interaction with a colliding pulse, highlighting the reduction of polarization due to stochastic heating. Laser parameters were $a_0 = 2.5$, $w_0 = 20\,\mu\text{m}$, $w_1 = 5\,\mu\text{m}$.

$\mathcal{H} = \text{const}$ along an electron orbit, as shown in Fig. 2(a). An electron in an *untrapped* orbit [black dashed line in Fig. 2(a)], where it simply passes the plasma wave, can move to a *trapped* orbit [black solid line in Fig. 2(a)] where it is accelerated inside the plasma wave by gaining momentum. The interference of the driver and collider laser with peak normalized vector potentials $a_0 > a_1$, respectively, creates a standing ($v_{ph} = 0$) beat wave causing the stochastic heating of electrons [45–48]. The longitudinal momentum p_z gained in the heating process enables some electrons to become trapped in the plasma wave [28–30,48]. In Fig. 2(b) the longitudinal momentum distribution of electrons is shown for varying colliding pulse strengths, showing how increasing a_1 causes more heating, resulting in a larger fraction of electrons gaining higher amounts of p_z. The theoretical framework of spin-polarized bunch injection in CPI is developed in more detail in Ref. [44].

To study the electron spin evolution in CPI, the Thomas-Bargmann-Michel-Telegdi equation [49] describing the spin dynamics of electrons can be used. The spin vector $\boldsymbol{s}$ of unit length evolves according to classical spin dynamics in time-varying electric and magnetic fields as

$$\frac{d\boldsymbol{s}}{dt} = (\boldsymbol{\Omega_T} + \boldsymbol{\Omega_a}) \times \boldsymbol{s}, \tag{1}$$

with

$$\boldsymbol{\Omega_T} = \frac{q_e}{m_e}\left(\frac{1}{\gamma_e}\boldsymbol{B} - \frac{\boldsymbol{\beta}}{1+\gamma_e} \times \frac{\boldsymbol{E}}{c}\right), \tag{2a}$$

$$\boldsymbol{\Omega_a} = a_e \frac{q_e}{m_e}\left[\boldsymbol{B} - \frac{\gamma_e}{1+\gamma_e}\boldsymbol{\beta}(\boldsymbol{\beta}\cdot\boldsymbol{B}) - \boldsymbol{\beta} \times \frac{\boldsymbol{E}}{c}\right], \tag{2b}$$

where $\gamma_e = 1/\sqrt{1-\beta^2}$ is the Lorentz factor of the electron, $\boldsymbol{\beta} = \boldsymbol{v}/c$ is the normalized velocity, and m_e, $-q_e$, and $a_e \approx 1.16 \times 10^{-3}$ are the electron mass, charge, and anomalous magnetic moment, respectively. Given that the spin precession rate depends on $\boldsymbol{\beta}$, it is clear that the chaotic motion due to stochastic heating in the standing beat wave also results in stochastic evolution of the spin vector $\boldsymbol{s}$. This causes a fraction of initially polarized (e.g., along $\hat{\boldsymbol{e}}_z$) electrons to become depolarized, as shown in Fig. 2(c), highlighting how the stochastic heating from increasing a_1 results in a larger amount of depolarized electrons. Unlike in the previously published regimes [18,19,50], where the spins precess due to the strong azimuthal fields on the periphery of the bubble, in CPI the depolarization is a result of stochastic effects, as discussed in depth in another publication [44]. In CPI, the stochastic spin depolarization of the injected electrons can be suppressed by varying a_1 and w_1, while injecting close to the axis inherently avoids strongly depolarizing azimuthal B fields; z_c can be varied to optimize energy gain and energy spread of the bunch. These additional degrees of freedom enable CPI to be used to generate highly polarized, high-quality electron bunches from prepolarized plasma targets.

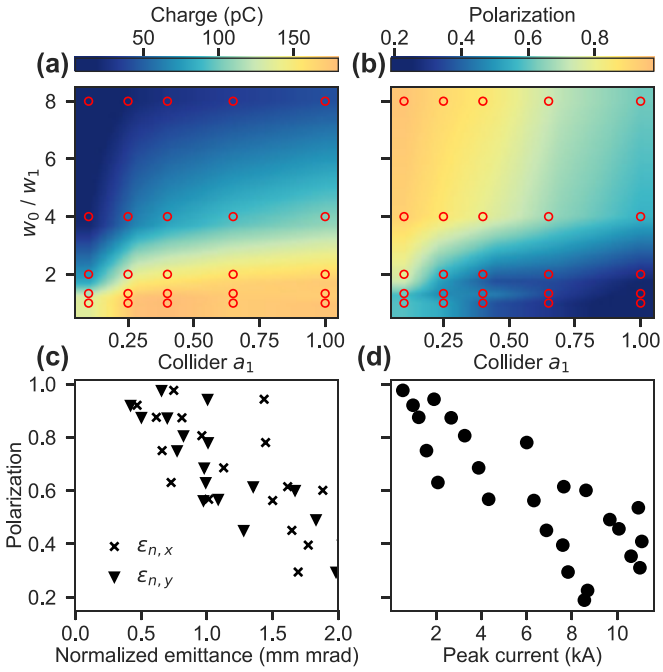

FIG. 3. Variation of spin-polarized electron beam parameters. (a) Charge and (b) polarization as a function of a_1 and w_1 with $w_0 = 20\,\mu\text{m}$ and $a_0 = 2.5$. The red circles denote individual simulation results while the color scale is an interpolation over these points. (c) The normalized emittance and polarization of the generated beams. (d) Peak current and polarization variation.

III. SIMULATIONS OF POLARIZED COLLIDING PULSE INJECTION

We used the quasi-three-dimensional (3D) particle-in-cell code FBPIC [51,52] to study the generation of polarized electron beams using CPI. The code was modified to include the particles' spin properties [44] by implementing Eq. (1). Other spin effects were not modeled [53] as the Stern-Gerlach force is orders of magnitude smaller than the Lorentz force [50] and the timescale for the Sokolov-Ternov effect [11], even in the hundreds of GV/m field strengths present in LPAs, is on the order of microseconds, being much longer than the typical nanosecond duration of laser-plasma acceleration [54]. Scaling of the electron bunch spin polarization in CPI was studied by performing a 2D grid scan varying the focal spot size w_1 and a_1 of the colliding laser. Both lasers had a full width at half maximum (FWHM) pulse duration of 30 fs and $\lambda_0 = 800\,\text{nm}$. The plasma density profile in the simulations consisted of a 50-μm linear ramp followed by a plateau with $n_e = 1 \times 10^{18}\,\text{cm}^{-3}$. The simulation box had a length of 70 μm and a radius of 60 μm with 3000 and 500 cells, respectively, and moved in the positive z direction at the speed of light. The number of particles per cell was set to two, two, and four for the longitudinal, radial, and azimuthal directions, respectively, with three azimuthal modes used. The colliding laser was injected backwards from an antenna and was set to collide with the driver laser at $z = 100\,\mu\text{m}$, which was also the focal plane for both the driver and collider laser. A fully prepolarized and preionized plasma was modeled, with the initial spin vector of the background electrons set to $\boldsymbol{s} = \hat{\boldsymbol{e}}_z$. The electron beam parameters were analyzed after propagating the driver beam through 500 μm of plasma, with the polarization calculated as $P = |\Sigma_i^N \boldsymbol{s}_i/N|$.

Results of this scan are depicted in Fig. 3, highlighting that even without careful optimization, CPI allows highly polarized bunches with submicron normalized emittance to be generated. Figures 3(a) and 3(b) show that larger w_1 as well as increased a_1 generate bunches with a higher charge at the expense of spin polarization. This occurs as both a larger focal spot size w_1 and higher intensity a_1 lead to a larger volume of background electrons being stochastically heated, leading to a larger fraction of electrons to become substantially depolarized. Thus, highly polarized beams $P > 70\%$ are generated employing moderate collider laser intensities $a_1 \leqslant 0.5$ and small collider spot sizes relative to the driver laser. Figure 3(c) shows that normalized emittance on the order of 1 mm mrad can be expected, especially for beams with high polarization in the range of 60%–100%. The bunch charge is up to 50 pC for beams with polarization as high as 90 %; correspondingly, peak currents of several kiloamperes are reached, as depicted in Fig. 3(d).

These results vastly outperform previously proposed schemes for LPA-generated polarized beams, both for the case of DDR [17,19] and self-injection [18], particularly in terms of the generated bunch charge. We also note that in Ref. [19], the longitudinal polarization of a Gaussian electron beam was calculated to vary as $P = \text{sinc}(0.0072 I_{\text{peak}})$, meaning a fully depolarized beam $P = 0$ would be expected for $I_{\text{peak}} = 4.5\,\text{kA}$. This limitation is, however, derived from and inherently linked to the density down-ramp profile used in that study. From our work it is clear that highly polarized, high-current electron bunches can indeed be generated using Gaussian laser pulses.

IV. BAYESIAN OPTIMIZATION OF POLARIZED COLLIDING PULSE INJECTION

The use of the colliding laser pulse to inject electrons introduces several free parameters that can be tuned to generate electron bunches with desired application-specific parameters. Together with the driver laser and plasma properties, this spans a large, multidimensional parameter space. Recent work has shown that Bayesian optimization (BO) algorithms are very well suited for finding the optimal parameters for such multidimensional problems [31,32]. We used the BO toolkit OPTIMAS [55,56] to optimize a set of easily adjustable input parameters to generate electron bunches with high charge, low-energy spread, and high longitudinal polarization. In these FBPIC simulations, the plasma profile consisted of a 100-μm-long linear ramp starting at $z = 0$ followed by a density plateau with n_e. The varying (*to be optimized*) parameters (cf. Fig. 1) were the collider intensity a_1, the collision point of the laser pulses z_c, the focal plane z_f (overlapping for both lasers, i.e., $z_f = z_{f,0} = z_{f,1}$), the plasma density n_e, and the driver intensity a_0. A fixed driver laser power $P_0 = 100\,\mathrm{TW}$ was used, thus the variation of a_0 also changed w_0 as $a_0^2 w_0^2 =$ const. The collider spot size was fixed at $w_1 = 5\,\mu\mathrm{m}$ and both pulses had a FWHM duration of 30 fs. The simulation box length was 60 μm with 3000 cells in the longitudinal direction, whereas the radius of the box was scaled to always be $r > 2.5 w_0$, with $\Delta r = 120\,\mathrm{nm}$. We note that in this optimization the key free experimental parameters were varied, i.e., these parameters would also be tuned in case of manual optimization.

The beam properties were analyzed within the plasma after propagating the driver laser pulse for 1 mm. The fitness function was set to $f = -\sqrt{Q E_m}/[\Delta E(1 - P)]$, where Q is the beam charge, E_m is the median energy, ΔE is the median absolute deviation of the energy, and P is the beam polarization. The BO was run for 100 iterations. Despite the use of only a limited set of varied parameters, the BO quickly converged on a parameter region that results in the generation of high-quality electron beams. The parameters for reaching the lowest f were $a_0 = 2.68$, $w_0 = 20.4\,\mu\mathrm{m}$, $z_f = 135.3\,\mu\mathrm{m}$, $z_c = 281.4\,\mu\mathrm{m}$, and $n_e = 8.2 \times 10^{17}\,\mathrm{cm}^{-3}$. The properties of the bunch resulting in the lowest value of f are presented in Table I, showing that electron bunches with a few percent energy spread, tens of picocoulomb of charge, and polarization of 90% are achievable given the reasonable laser parameters employed.

TABLE I. Properties of the bunch with lowest value of f achieved by BO of the polarized CPI scheme.

Beam parameter	Value	Unit
Mean energy	85.2	MeV
Energy spread (rms)	4.4	%
Peak current	3.6	kA
Bunch duration (rms)	3.8	fs
Charge	31.8	pC
Normalized emittance, x plane	0.90	mm mrad
Normalized emittance, y plane	0.84	mm mrad
Spin polarization	0.90	

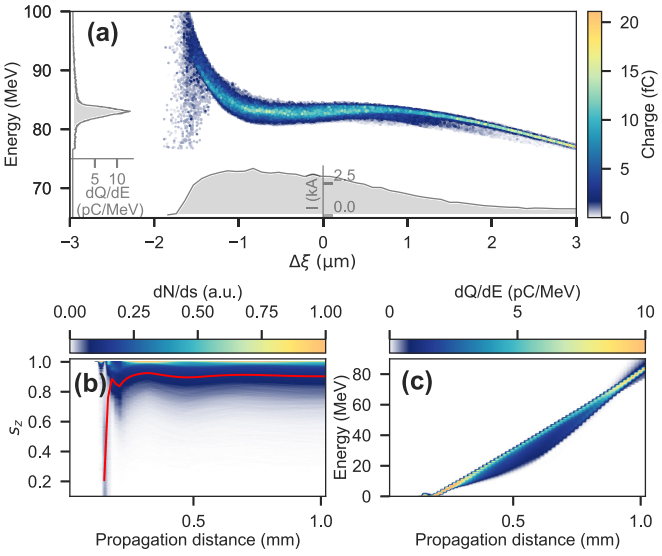

FIG. 4. Optimized highly polarized electron beam. (a) Longitudinal phase space of the beam. (b) Evolution of s_z during acceleration. The color scale shows the distribution of s_z while the red line is $P = \langle s_z \rangle$. (c) Evolution of beam energy.

The longitudinal phase space of the optimized beam is shown in Fig. 4(a), highlighting the flattened energy distribution. The evolution of the longitudinal spin component of the accelerated electrons depicted in Fig. 4(b) indicates that the spin distribution and beam polarization is stable at ∼90 % after the electrons become highly relativistic, as has already been shown previously [17,57]. Consequently, the electron bunch energy could be increased by extending the acceleration length without significantly altering the beam polarization. As seen from Eq. (1), the spin precession depends only on applied fields, which suggests a lack of additional depolarization in the plasma outcoupling down ramp. This was confirmed by simulations of beam extraction from the plasma using emittance-conserving plasma down ramps [58]. The electron energy spectrum evolution depicted in Fig. 4(c) shows that the bunch is almost optimally beam loaded [59], while also indicating that dephasing or depletion are not yet limiting the energy gain. The 100-TW class lasers have already been used to demonstrate multi-GeV energy gains [60,61], suggesting the electron beam energy could be extended to GeV and beyond in a sufficiently long plasma source.

We note that the optimization presented above can be further improved upon in the future, e.g., by allowing w_1 or the focal plane of the collider laser to be changed. Additionally, the transverse or temporal profile of the collider laser could be varied to create tailored bunch spatial or current profiles. For example, a radially flattened beat-wave pattern arising from an annular collider pulse could potentially further increase the injected charge while maintaining the high polarization levels demonstrated in this work. Overall, CPI shows great potential to produce high-quality and high-current polarized electron beams required for a host of applications.

The results above assume a fully prepolarized plasma $\bar{s}_z = 1$, which may be difficult to achieve experimentally. Simulations using optimized parameters leading to beams depicted

in Fig. 4 were carried out to study the final beam polarization P dependence on the initial plasma prepolarization $\bar{s}_z$. A constant depolarization of 0.9 was found for $\bar{s}_z = [0.3, 1]$. Therefore, our results demonstrating low depolarization will be instrumental in near-term experimental demonstrations for spin-polarized LPA, even if performed with lower initial prepolarization.

V. CONCLUSION

In summary, we show that narrow energy spread, low emittance, and highly polarized electron bunches can be generated using CPI in a prepolarized plasma source. The additional degrees of freedom in CPI enable precise control of the injection process and subsequent beam loading, all the while allowing high spin polarization of the bunch to be retained. Our work represents orders of magnitude improvements of the delivered beam charge while retaining high polarization upon previous results, bringing the advent of high-current polarized LPAs to within reach of currently commissioned laser systems. A CPI-based, compact, thoroughly tunable source of highly polarized electron beams is a very promising candidate for injectors at future storage rings or linear collider setups or as an injector upgrade for existing polarized storage rings [62]. Further, LPA employing polarized CPI represents a long-awaited tool to expand access to scientific and industrial applications requiring polarized particle beams.

ACKNOWLEDGMENTS

The authors acknowledge funding from the DESY Strategy Fund. This work was supported by the Maxwell computational resources at DESY. The authors gratefully acknowledge the Gauss Centre for Supercomputing e.V. [63] for funding this project by providing computing time through the John von Neumann Institute for Computing (NIC) on the GCS Supercomputer JUWELS at Jülich Supercomputing Centre (JSC).

[1] H. A. Tolhoek, Electron polarization, theory and experiment, Rev. Mod. Phys. **28**, 277 (1956).
[2] K. Abe *et al.* (E143 Collaboration), Precision Measurement of the Deuteron Spin Structure Function g_1^d, Phys. Rev. Lett. **75**, 25 (1995).
[3] P. L. Anthony *et al.* (SLAC E158 Collaboration), Observation of Parity Nonconservation in Møller Scattering, Phys. Rev. Lett. **92**, 181602 (2004).
[4] B. S. Schlimme, P. Achenbach, C. A. Ayerbe Gayoso, J. C. Bernauer, R. Bohm, D. Bosnar, T. Challand, M. O. Distler, L. Doria, F. Fellenberger *et al.*, Measurement of the Neutron Electric to Magnetic Form Factor Ratio at $Q^2 = 1.58$ GeV^2 using the Reaction $^3\vec{\mathrm{He}}(\vec{e}, e'n)pp$, Phys. Rev. Lett. **111**, 132504 (2013).
[5] D. Androić *et al.* (The Jefferson Lab Qweak Collaboration), Precision measurement of the weak charge of the proton, Nature (London) **557**, 207 (2018).
[6] V. Shiltsev and F. Zimmermann, Modern and future colliders, Rev. Mod. Phys. **93**, 015006 (2021).
[7] G. Moortgat-Pick, T. Abe, G. Alexander, B. Ananthanarayan, A. A. Babich, V. Bharadwaj, D. Barber, A. Bartl, A. Brachmann, S. Chen *et al.*, Polarized positrons and electrons at the linear collider, Phys. Rep. **460**, 131 (2008).
[8] R. Märtin, G. Weber, R. Barday, Y. Fritzsche, U. Spillmann, W. Chen, R. D. Dubois, J. Enders, M. Hegewald, S. Hess *et al.*, Polarization Transfer of Bremsstrahlung Arising from Spin-Polarized Electrons, Phys. Rev. Lett. **108**, 264801 (2012).
[9] D. Abbott *et al.* (PEPPo Collaboration), Production of Highly Polarized Positrons Using Polarized Electrons at MeV Energies, Phys. Rev. Lett. **116**, 214801 (2016).
[10] P. J. Schultz and K. G. Lynn, Interaction of positron beams with surfaces, thin films, and interfaces, Rev. Mod. Phys. **60**, 701 (1988).
[11] A. A. Sokolov and I. M. Ternov, Synchrotron radiation, Sov. Phys. J. **10**, 39 (1967).
[12] D. T. Pierce, F. Meier, and P. Zürcher, Negative electron affinity GaAs: A new source of spin-polarized electrons, Appl. Phys. Lett. **26**, 670 (1975).
[13] T. Tajima and J. M. Dawson, Laser Electron Accelerator, Phys. Rev. Lett. **43**, 267 (1979).
[14] E. Esarey, C. B. Schroeder, and W. P. Leemans, Physics of laser-driven plasma-based electron accelerators, Rev. Mod. Phys. **81**, 1229 (2009).
[15] H. Batelaan, A. S. Green, B. A. Hitt, and T. J. Gay, Optically Pumped Electron Spin Filter, Phys. Rev. Lett. **82**, 4216 (1999).
[16] M. M. Dellweg and C. Müller, Spin-Polarizing Interferometric Beam Splitter for Free Electrons, Phys. Rev. Lett. **118**, 070403 (2017).
[17] M. Wen, M. Tamburini, and C. H. Keitel, Polarized Laser-WakeField-Accelerated Kiloampere Electron Beams, Phys. Rev. Lett. **122**, 214801 (2019).
[18] H. C. Fan, X. Y. Liu, X. F. Li, J. F. Qu, Q. Yu, Q. Kong, S. M. Weng, M. Chen, M. Büscher, P. Gibbon *et al.*, Control of electron beam polarization in the bubble regime of laser-wakefield acceleration, New J. Phys. **24**, 083047 (2022).
[19] Y. Wu, L. Ji, X. Geng, Q. Yu, N. Wang, B. Feng, Z. Guo, W. Wang, C. Qin, X. Yan *et al.*, Polarized electron-beam acceleration driven by vortex laser pulses, New J. Phys. **21**, 073052 (2019).
[20] Y. Wu, L. Ji, X. Geng, Q. Yu, N. Wang, B. Feng, Z. Guo, W. Wang, C. Qin, X. Yan *et al.*, Polarized electron acceleration in beam-driven plasma wakefield based on density down-ramp injection, Phys. Rev. E **100**, 043202 (2019).
[21] Z. Nie, F. Li, F. Morales, S. Patchkovskii, O. Smirnova, W. An, N. Nambu, D. Matteo, K. A. Marsh, F. Tsung *et al.*, *In Situ* Generation of High-Energy Spin-Polarized Electrons in a Beam-Driven Plasma Wakefield Accelerator, Phys. Rev. Lett. **126**, 054801 (2021).
[22] Z. Nie, F. Li, F. Morales, S. Patchkovskii, O. Smirnova, W. An, C. Zhang, Y. Wu, N. Nambu, D. Matteo *et al.*, Highly spin-polarized multi-GeV electron beams generated by single-species plasma photocathodes, Phys. Rev. Res. **4**, 033015 (2022).
[23] D. Del Sorbo, D. Seipt, T. G. Blackburn, A. G. R. Thomas, C. D. Murphy, J. G. Kirk, and C. P. Ridgers, Spin polarization

of electrons by ultraintense lasers, Phys. Rev. A **96**, 043407 (2017).
[24] Y.-F. Li, R. Shaisultanov, K. Z. Hatsagortsyan, F. Wan, C. H. Keitel, and J.-X. Li, Ultrarelativistic Electron-Beam Polarization in Single-Shot Interaction with an Ultraintense Laser Pulse, Phys. Rev. Lett. **122**, 154801 (2019).
[25] D. Seipt, D. Del Sorbo, C. P. Ridgers, and A. G. R. Thomas, Ultrafast polarization of an electron beam in an intense bichromatic laser field, Phys. Rev. A **100**, 061402(R) (2019).
[26] K. Xue, R.-T. Guo, F. Wan, R. Shaisultanov, Y.-Y. Chen, Z.-F. Xu, X.-G. Ren, K. Z. Hatsagortsyan, C. H. Keitel, and J.-X. Li, Generation of arbitrarily polarized GeV lepton beams via nonlinear Breit-Wheeler process, Fundam. Res. **2**, 539 (2022).
[27] Y.-F. Li, Y.-Y. Chen, K. Z. Hatsagortsyan, and C. H. Keitel, Helicity Transfer in Strong Laser Fields via the Electron Anomalous Magnetic Moment, Phys. Rev. Lett. **128**, 174801 (2022).
[28] D. Umstadter, J. K. Kim, and E. Dodd, Laser Injection of Ultrashort Electron Pulses into Wakefield Plasma Waves, Phys. Rev. Lett. **76**, 2073 (1996).
[29] E. Esarey, R. F. Hubbard, W. P. Leemans, A. Ting, and P. Sprangle, Electron Injection into Plasma Wakefields by Colliding Laser Pulses, Phys. Rev. Lett. **79**, 2682 (1997).
[30] J. Faure, C. Rechatin, A. Norlin, A. Lifschitz, Y. Glinec, and V. Malka, Controlled injection and acceleration of electrons in plasma wakefields by colliding laser pulses, Nature (London) **444**, 737 (2006).
[31] R. J. Shalloo, S. J. D. Dann, J.-N. Gruse, C. I. D. Underwood, A. F. Antoine, C. Arran, M. Backhouse, C. D. Baird, M. D. Balcazar, N. Bourgeois *et al.*, Automation and control of laser wakefield accelerators using Bayesian optimization, Nat. Commun. **11**, 6355 (2020).
[32] S. Jalas, M. Kirchen, P. Messner, P. Winkler, L. Hübner, J. Dirkwinkel, M. Schnepp, R. Lehe, and A. R. Maier, Bayesian Optimization of a Laser-Plasma Accelerator, Phys. Rev. Lett. **126**, 104801 (2021).
[33] T. P. Rakitzis, P. C. Samartzis, R. L. Toomes, T. N. Kitsopoulos, A. Brown, G. G. Balint-Kurti, O. S. Vasyutinskii, and J. A. Beswick, Spin-polarized hydrogen atoms from molecular photodissociation, Science **300**, 1936 (2003).
[34] T. P. Rakitzis, Pulsed-laser production and detection of spin-polarized hydrogen atoms, Chem. Phys. Chem. **5**, 1489 (2004).
[35] D. Sofikitis, L. Rubio-Lago, A. J. Alexander, and T. P. Rakitzis, Nanosecond control and high-density production of spin-polarized hydrogen atoms, Europhys. Lett. **81**, 68002 (2008).
[36] D. Sofikitis, P. Glodic, G. Koumarianou, H. Jiang, L. Bougas, P. C. Samartzis, A. Andreev, and T. P. Rakitzis, Highly Nuclear-Spin-Polarized Deuterium Atoms from the UV Photodissociation of Deuterium Iodide, Phys. Rev. Lett. **118**, 233401 (2017).
[37] D. Sofikitis, C. S. Kannis, G. K. Boulogiannis, and T. P. Rakitzis, Ultrahigh-Density Spin-Polarized H and D Observed via Magnetization Quantum Beats, Phys. Rev. Lett. **121**, 083001 (2018).
[38] A. Hützen, J. Thomas, J. Böker, R. Engels, R. Gebel, A. Lehrach, A. Pukhov, T. P. Rakitzis, D. Sofikitis, and M. Büscher, Polarized proton beams from laser-induced plasmas, High Power Laser Sci. Eng. **7**, e16 (2019).
[39] A. K. Spiliotis, M. Xygkis, M. E. Koutrakis, K. Tazes, G. K. Boulogiannis, C. S. Kannis, G. E. Katsoprinakis, D. Sofikitis, and T. P. Rakitzis, Ultrahigh-density spin-polarized hydrogen isotopes from the photodissociation of hydrogen halides: New applications for laser-ion acceleration, magnetometry, and polarized nuclear fusion, Light: Sci. Appl. **10**, 35 (2021).
[40] T. P. Rakitzis (private communication).
[41] L. Drescher, O. Kornilov, T. Witting, V. Shokeen, M. J. Vrakking, and B. Schütte, Extreme-ultraviolet spectral compression by four-wave mixing, Nat. Photon. **15**, 263 (2021).
[42] S. Bohlen, T. Brümmer, F. Grüner, C. A. Lindstrøm, M. Meisel, T. Staufer, M. J. V. Streeter, M. C. Veale, J. C. Wood, R. D'Arcy *et al.*, *In Situ* Measurement of Electron Energy Evolution in a Laser-Plasma Accelerator, Phys. Rev. Lett. **129**, 244801 (2022).
[43] E. Esarey and M. Pilloff, Trapping and acceleration in nonlinear plasma waves, Phys. Plasmas **2**, 1432 (1995).
[44] Z. Gong, M. Quin, S. Bohlen, C. H. Keitel, K. Põder, and M. Tamburini, Spin-polarized electron beam generation in the colliding-pulse injection scheme, arXiv:2303.16966 [Matter Radiat. Extremes (to be published)].
[45] J. T. Mendonça, Threshold for electron heating by two electromagnetic waves, Phys. Rev. A **28**, 3592 (1983).
[46] P. Zhang, N. Saleh, S. Chen, Z. M. Sheng, and D. Umstadter, Laser-Energy Transfer and Enhancement of Plasma Waves and Electron Beams by Interfering High-Intensity Laser Pulses, Phys. Rev. Lett. **91**, 225001 (2003).
[47] A. Bourdier, D. Patin, and E. Lefebvre, Stochastic heating in ultra high intensity laser-plasma interaction, Physica D **206**, 1 (2005).
[48] V. Malka, J. Faure, C. Rechatin, A. Ben-Ismail, J. K. Lim, X. Davoine, and E. Lefebvre, Laser-driven accelerators by colliding pulses injection: A review of simulation and experimental results, Phys. Plasmas **16**, 056703 (2009).
[49] V. Bargmann, L. Michel, and V. L. Telegdi, Precession of the Polarization of Particles Moving in a Homogeneous Electromagnetic Field, Phys. Rev. Lett. **2**, 435 (1959).
[50] M. Wen, C. H. Keitel, and H. Bauke, Spin-one-half particles in strong electromagnetic fields: Spin effects and radiation reaction, Phys. Rev. A **95**, 042102 (2017).
[51] R. Lehe, M. Kirchen, I. A. Andriyash, B. B. Godfrey, and J. L. Vay, A spectral, quasi-cylindrical and dispersion-free particle-in-cell algorithm, Comput. Phys. Commun. **203**, 66 (2016).
[52] S. Jalas, I. Dornmair, R. Lehe, H. Vincenti, J. L. Vay, M. Kirchen, and A. R. Maier, Accurate modeling of plasma acceleration with arbitrary order pseudo-spectral particle-in-cell methods, Phys. Plasmas **24**, 033115 (2017).
[53] S. R. Mane, Y. M. Shatunov, and K. Yokoya, Spin-polarized charged particle beams in high-energy accelerators, Rep. Prog. Phys. **68**, 1997 (2005).
[54] J. Thomas, A. Hützen, A. Lehrach, A. Pukhov, L. Ji, Y. Wu, X. Geng, and M. Büscher, Scaling laws for the depolarization time of relativistic particle beams in strong fields, Phys. Rev. Accel. Beams **23**, 064401 (2020).
[55] A. F. Pousa, S. Jalas, M. Kirchen, A. M. de la Ossa, M. Thévenet, S. Hudson, J. Larson, A. Huebl, J. L. Vay, and R. Lehe, Multitask optimization of laser-plasma accelerators using simulation codes with different fidelities, in *Proceedings of the 13th International Particle Accelerator Conference* (JACoW, 2022), pp. 1761–1764.
[56] A. F. Pousa, S. Jalas, M. Kirchen, A. M. de la Ossa, M. Thévenet, S. Hudson, J. Larson, A. Huebl, J. L. Vay, and R. Lehe, Bayesian optimization of laser-plasma accelerators

assisted by reduced physical models, Phys. Rev. Accel. Beams **26**, 084601 (2023).

[57] J. Vieira, C. K. Huang, W. B. Mori, and L. O. Silva, Polarized beam conditioning in plasma based acceleration, Phys. Rev. ST Accel. Beams **14**, 071303 (2011).

[58] I. Dornmair, K. Floettmann, and A. R. Maier, Emittance conservation by tailored focusing profiles in a plasma accelerator, Phys. Rev. ST Accel. Beams **18**, 041302 (2015).

[59] M. Kirchen, S. Jalas, P. Messner, P. Winkler, T. Eichner, L. Hübner, T. Hülsenbusch, L. Jeppe, T. Parikh, M. Schnepp *et al.*, Optimal Beam Loading in a Laser-Plasma Accelerator, Phys. Rev. Lett. **126**, 174801 (2021).

[60] C. E. Clayton, J. E. Ralph, F. Albert, R. A. Fonseca, S. H. Glenzer, C. Joshi, W. Lu, K. A. Marsh, S. F. Martins, W. B. Mori *et al.*, Self-Guided Laser Wakefield Acceleration beyond 1 GeV Using Ionization-Induced Injection, Phys. Rev. Lett. **105**, 105003 (2010).

[61] M. Mirzaie, S. Li, M. Zeng, N. A. M. Hafz, M. Chen, G. Y. Li, Q. J. Zhu, H. Liao, T. Sokollik, F. Liu *et al.*, Demonstration of self-truncated ionization injection for GeV electron beams, Sci. Rep. **5**, 14659 (2015).

[62] W. Hillert, A. Balling, O. Boldt, A. Dieckmann, M. Eberhardt, F. Frommberger, D. Heiliger, N. Heurich, R. Koop, F. Klarner *et al.*, Beam and spin dynamics in the fast ramping storage ring ELSA: Concepts and measures to increase beam energy, current and polarization, EPJ Web Conf. **134**, 05002 (2017).

[63] www.gauss-centre.eu.